

# High Reynolds number experimentation in the US Navy's William B Morgan Large Cavitation Channel

Robert J Etter<sup>1</sup>, J Michael Cutbirth<sup>2</sup>, Steven L Ceccio<sup>3</sup>,  
David R Dowling<sup>3</sup> and Marc Perlin<sup>4</sup>

<sup>1</sup> Naval Surface Warfare Center Carderock Division, 9500 MacArthur Boulevard,  
West Bethesda, MD 20817, USA

<sup>2</sup> Naval Surface Warfare Center Memphis Detachment, 2700 Channel Avenue, Memphis,  
TN 38113, USA

<sup>3</sup> Department of Mechanical Engineering, University of Michigan, Ann Arbor, MI 48109,  
USA

<sup>4</sup> Department of Naval Architecture and Marine Engineering, University of Michigan,  
Ann Arbor, MI 48109, USA

Received 30 September 2004, in final form 13 April 2005

Published 25 July 2005

Online at [stacks.iop.org/MST/16/1701](http://stacks.iop.org/MST/16/1701)

## Abstract

The William B Morgan Large Cavitation Channel (LCC) is a large variable-pressure closed-loop water tunnel that has been operated by the US Navy in Memphis, TN, USA, since 1991. This facility is well designed for a wide variety of hydrodynamic and hydroacoustic tests. Its overall size and capabilities allow test-model Reynolds numbers to approach, or even achieve, those of full-scale air- or water-borne transportation systems. This paper describes the facility along with some novel implementations of measurement techniques that have been successfully utilized there. In addition, highlights are presented from past test programmes involving (i) cavitation, (ii) near-zero pressure-gradient turbulent boundary layers, (iii) the near-wake flow characteristics of a two-dimensional hydrofoil and (iv) a full-scale research torpedo.

**Keywords:** flow testing at high pressure, high temperature, high Reynolds number

(Some figures in this article are in colour only in the electronic version)

## 1. Introduction

This paper describes the William B Morgan Large Cavitation Channel (LCC) and some of the attendant instrumentation that has been used there for high Reynolds number tests. It is intended to concisely convey the wide range of experimentation that is possible at high Reynolds numbers in the LCC. No single prior report on the LCC contains all the material presented here, and in addition, some new experimental results are provided to illustrate recent research conducted in the LCC.

Plans for the LCC began in 1982 at the US Naval Surface Warfare Center (NSWC). From the beginning, it was designed to be sufficiently large so that Reynolds number scaling of

model test results to full-scale devices or prototypes would either be unnecessary or at most would involve an extrapolation of only one order of magnitude or so. Approximately 10 years later, the facility was operational. After a decade of use, it was renamed on 27 April 2001, for retired NSWC engineer and hydrodynamicist, Dr William B Morgan, a leader in the effort to make this facility a reality.

The LCC was designed to be a modern hydrodynamic and hydroacoustic test facility (Etter and Wilson 1992, Etter 2001). Although its size makes it unique, it also combines much of the best water tunnel engineering available and has the necessary supporting and auxiliary systems for testing complete powered hull-propulsor-appendage systems. Furthermore, the LCC's main drive system, turning vanes, flow management section

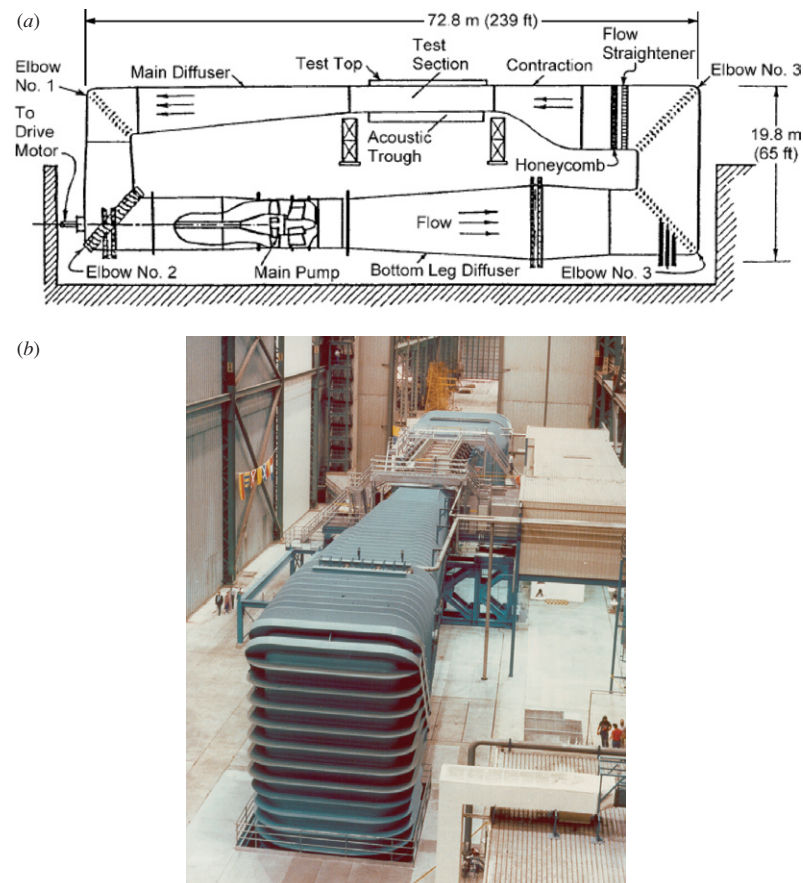


**Figure 1.** Schematic of the William B Morgan Large Cavitation Channel (a) and a picture of the LCC overlooking the diffuser (b). Note the size of the people at the left and right edges of the photograph.

and physical construction were all designed to provide low-turbulence uniform flow in the test section with minimal background noise. Overall, the facility has met its performance targets, and test results from the LCC have led to quieter more efficient ship designs, and upgrades and design alterations for existing ships. In addition, the LCC is an exceptional facility for basic hydromechanics and hydrodynamics research. The specifications and capabilities of the LCC are discussed in the next section.

Traditional and modern flow diagnostics have been used in the LCC. This includes both single- and multi-component fluid velocity measurements via laser Doppler velocimetry (LDV) and particle-imaging velocimetry (PIV). Here, the long beam-paths in particle-laden water produce experimental challenges that are not encountered in smaller test facilities. Tunnel sidewall or model-surface measurements—for static and dynamic pressure and shear stress, radiated sound, and surface-normal accelerations—have been achieved with both commercial and custom-fabricated instrumentation. The primary hardware challenge is long-duration underwater service at elevated and/or reduced static pressure. Section 3 describes the specialized LDV and PIV equipment used at the LCC along with descriptions of the shear-stress and hydroacoustic instrumentation.

Tests conducted at the LCC have included both surface-ship and submerged-vessel hull forms with propulsion systems, a suite of axisymmetric bodies, a two-dimensional hydrofoil and a large flat plate. Typically, hull form and

axisymmetric models are mounted on the removable test section top via one or more struts. However, two-dimensional test-section-spanning models have been supported by metal mounting plates that replace two or more of the LCC's many test section windows. Sample results from several of these studies are presented in section 4, while the final section describes future uses and possible upgrades for higher speed testing in the LCC.

## 2. LCC specifications and performance

The LCC is currently the world's largest low-turbulence variable-pressure closed-circuit water tunnel. It has an overall length and height of 72.8 m and 19.8 m, respectively, and water volume of 5300 m<sup>3</sup>. A schematic and a photograph of this facility are shown in figure 1. The LCC resides within a high-ceiling shop area with independent 100 and 75 ton overhead cranes that service the test section and extensive model preparation areas. The upper half of the LCC rises above ground level with the lower portion of the flow loop occupying a reinforced concrete trench. The LCC's structural shell and entire test section were fabricated from 304L stainless steel. External stiffening ribs and other supports are painted SA 516 carbon steel. Interior surfaces of the contraction, test section and diffuser were polished to about a 7  $\mu\text{m}$  finish. Other interior surfaces in the lower velocity regions of the flow circuit were not polished.

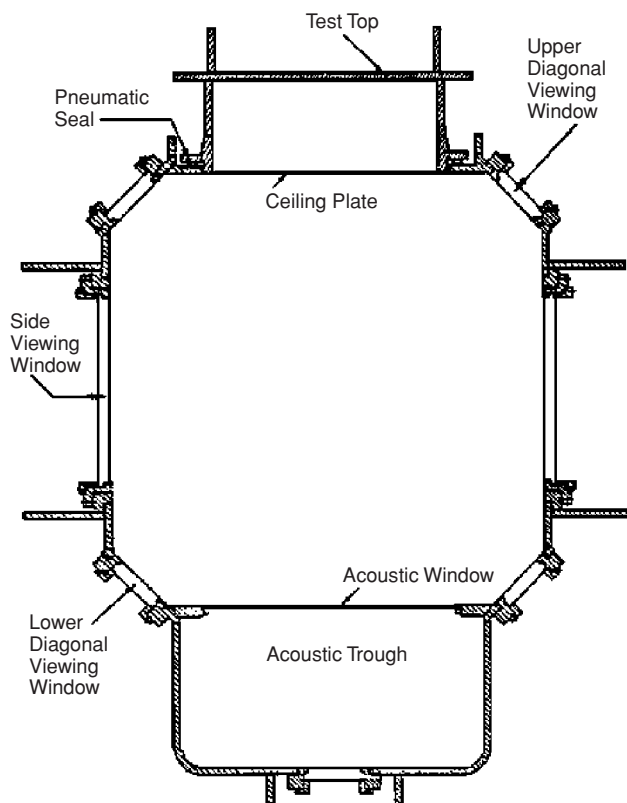


**Figure 2.** LCC test section cross section. The side-to-side and floor-to-ceiling dimensions are both 3.05 m.

The basic flow-loop design incorporates a flat interior ceiling such that the inside top of the contraction, test section and diffuser are all in the same horizontal plane. This design allows the hydrostatic pressure acting in the test section to be minimized for cavitation testing. To facilitate this flow-loop geometry, while achieving uniform flow in the LCC's test section, the six-to-one contraction upstream of the test section was designed to be asymmetric. The final contraction contours were selected after model tests (Wetzel and Arndt 1994a) confirmed uniform flow in the test section. The flow that enters the contraction first passes through a 610 mm long flow straightener with 102 mm square cells, and then through a 483 mm long hexagonal honeycomb having a cross-cell flat-to-flat dimension of 5.6 mm.

The LCC test section is 13 m long and has a nominal cross section of 3.05 m  $\times$  3.05 m ( $\pm 4$  or 5 mm). The corners of the test section are chamfered to create fillets (see figure 2) that inhibit the formation of streamwise (longitudinal) corner vortices. With this cross-sectional area, an axisymmetric model with 1 m diameter causes less than 10% blockage. The test section has 32 optical quality primary windows (1.17 m high, 0.54 m wide and 9.5 cm thick) and twice as many smaller windows mounted in the corner fillets (these windows are visible in figures 5 and 12). Test section access is possible through a personnel access hatch and via a removable test section top that is held in place with 16 motor-actuated latches. The test top is mated to the rest of the test section with alignment pins and an inflatable seal. The most common scheme for mounting models in the LCC is to secure the model to the removable top when both reside in a model preparation area and then transfer them together using one of the overhead

cranes to the LCC test section. In addition, flow tests with the test section top removed are possible, but only at Froude numbers based on water depth of less than unity.

The remainder of the flow circuit includes four mitred elbows with internal turning vanes, the pump and stator housing, and the main and bottom diffusers. The main diffuser has an expanding square cross section with a horizontal top. Its lower boundary slopes downward at 5° and each of the two sidewalls angles outward at 2.6°. The down-flow leg at the motor drive end of the LCC incorporates a square to round transition. The rotor and stator reside in round sections and the bottom leg diffuser incorporates the change from round back to square cross section. Again, experimental tests on model-scale (1:14) tunnel components (Wetzel and Arndt 1994a, 1994b) were critical in confirming the final design.

At the present time, the LCC is powered by a 10.44 MW 24-pole synchronous motor with a variable-frequency cycloconverter drive. The maximum rated motor speed is 61 rpm at a drive frequency of 12.2 Hz ( $= (n/2)(\text{rpm}/60)$ , where  $n$  is the number of poles). This motor turns a single-stage axial flow pump composed of a 5.52 m diameter seven-bladed impeller and a nine-bladed stator with a hub ratio of 0.55. Global electrical power usage measurements place the fully operational LCC power draw at about 8.6 MW for an empty test section speed of 19.3 m s<sup>-1</sup>. Thus, there is approximately 20% reserve power capacity for model losses. Tunnel pressure is maintained by an independent pump-powered control loop that moves water between the LCC and a head control tank. An additional large storage tank allows the top leg of the tunnel to be drained to the test section floor to facilitate in-test-section model and instrumentation work without having to discard water. This final operational feature saves time, lowers utility costs and provides a means for saving expensive seed particles when these are used in LDV and PIV studies.

The LCC's hydrodynamic performance covers a broad range of speed and pressure. Empty test section flow speeds and pressures are routinely set from 0.5 m s<sup>-1</sup> to 18.0 m s<sup>-1</sup> and 3.5 kPa to 414 kPa (absolute), respectively. Here, static pressure is specified at the top of the downstream end of the test section. Extended tunnel operation beyond this envelope is possible, but has not been attempted yet. Water temperature is not controlled but is monitored and has varied between 15 °C and 44 °C with typical temperatures of 20–25 °C. Outside the test-section sidewall boundary layers, the LDV-measured mean flow in the test section is uniform to within  $\pm 1\%$  throughout the tunnel's speed range. LDV and constant temperature anemometry (CTA) measurements of the root-mean-square turbulence level,  $u'/U$ , at the centre of the test section are shown in figure 3 for flow speeds from 0.5 m s<sup>-1</sup> to 15 m s<sup>-1</sup>. The LCC's CTA-measured turbulence level lies at or below 0.5% throughout the measured speed range with a typical value of  $\sim 0.3\%$ . Additional information of this type is available in Blanton (1995a) and Park *et al* (2003). A thorough compendium of LCC test section flow measurements is available in Park *et al* (2002). The free and dissolved air content is an important parameter when conducting cavitation studies. The LCC is equipped with a de-aeration system whereby the gas content of the flowing water can be modified. The dissolved oxygen content of the

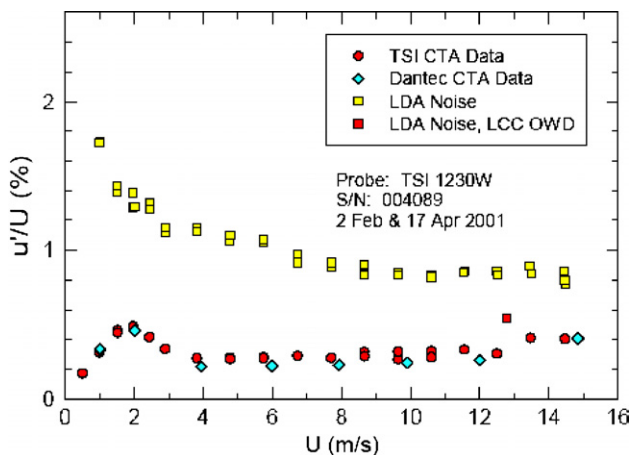


**Figure 3.** LCC test section turbulence level (root-mean-square velocity fluctuation divided by the average velocity) measured using LDV (aka LDA) and CTA techniques. The CTA measurements are considered to be more accurate.

tunnel water is continually monitored, and when necessary, the cavitation nuclei distribution can be measured with a cavitation susceptibility meter (CSM).

The LCC is also an acoustic test facility (Abbot *et al* 1993). Thus, the main pump components were designed to be free of cavitation. The primary motor is vibration isolated from the tunnel structure by two inline elastomeric drive couplings on the drive shaft that links the motor and the pump impeller, and via a two-stage inertial block system that supports the motor on a separate foundation from that which supports the tunnel structure. In addition, three of the four sets of turning vanes have acoustic treatments. The turning vanes upstream of the final elbow prior to the contraction were left untreated because they see the lowest flow velocity and are separated from the test section by the flow management section. When necessary, an additional noise control feature can be implemented in the lower portion of the LCC by filling the concrete trench with quiescent water. This improves the acoustical coupling between the LCC and its surroundings, thus allowing internal LCC sound to more easily radiate into the tunnel's foundation and the surrounding earth. The trench which contains 1.8 times the channel water volume serves a secondary function as a heat sink to reduce temperature rise during extended periods of high-speed testing.

Figure 4 shows the empty test section one-third-octave-band minimum-source-level noise floor of the LCC as determined by the nested hydrophone arrays described at the end of the next section. Here, source level is in decibels referenced to  $1 \mu\text{Pa}$  at a distance of 1 m over the design range of the arrays, 1–16 kHz, for test section speeds of  $2.6$ – $15.4 \text{ m s}^{-1}$ . These curves represent the minimum source level that can be measured by the LCC's hydrophone arrays for a point source at the centre of the test section in the absence of a model body. Higher level hydroacoustic sources present in the test section during model testing can be detected and quantified. The presence of a test body would slightly modify the figure 4 values. The data reported (Abbot *et al* 1993) are for the acquisition system status at that time. Computer and software upgrades to the system have occurred subsequently. The concrete trench was not filled with water for these measurements.

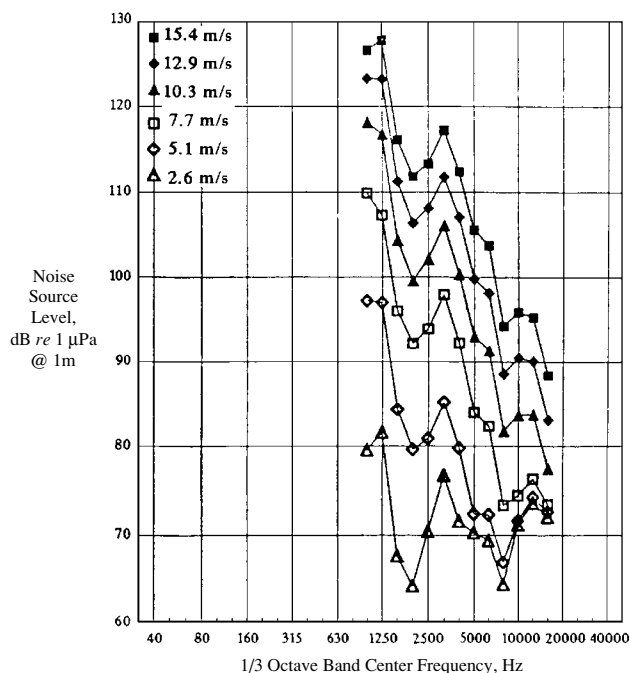


**Figure 4.** Empty-LCC-test-section background-noise equivalent source levels (in dB referenced to  $1 \mu\text{Pa}$  at a distance of 1 m) presented in 1/3 octave bands from 1 kHz to 16 kHz for test section flow speeds from  $2.6 \text{ m s}^{-1}$  to  $15.4 \text{ m s}^{-1}$ . Hydroacoustic sound sources with source levels higher than these curves can be quantified within the LCC. Quieter ones would fall within the background noise.

### 3. Instrumentation for the LCC

In its first 12 years of service, the LCC has hosted a wide variety of instrumentation for measuring fluid velocities, static and fluctuating pressures, water temperature, skin friction, radiated sound and many different integrated performance metrics for hydrodynamic devices: lift, drag, torque and mechanical power consumed or extracted. This section emphasizes unique instrumentation or unusual applications of common measurement techniques rather than providing a comprehensive list and description of the measurement techniques used in the LCC.

A principal purpose of the LCC is to conduct model-scale tests of hydrodynamic systems, including powered models. A series of force transmission dynamometers has been developed specifically for the LCC. These devices are operated in waterproof containers that can be placed within submerged test models. Five motors are available that deliver power up to 520 kW at 3500 rpm. Two of these motors can be operated in series for either co- or counter-rotating motion. Two additional motors are available that deliver up to 110 kW at 7200 rpm. Dynamometers are available that can measure drag and thrust up to 44 600 N and torque in either direction up to 677 N m. Hull models can be placed on the test section top and can be up to 12.2 m long with 1.5 m beam. Behind-hull propellers have been tested with diameters up to 450 mm. A strut-mounted pod system, shown in figure 5, is available for conducting open-water tests of powered propellers in a uniform flow. Planning is underway to modify this drive system to test propellers with much larger diameters, possibly as large as 1.4 m diameter.

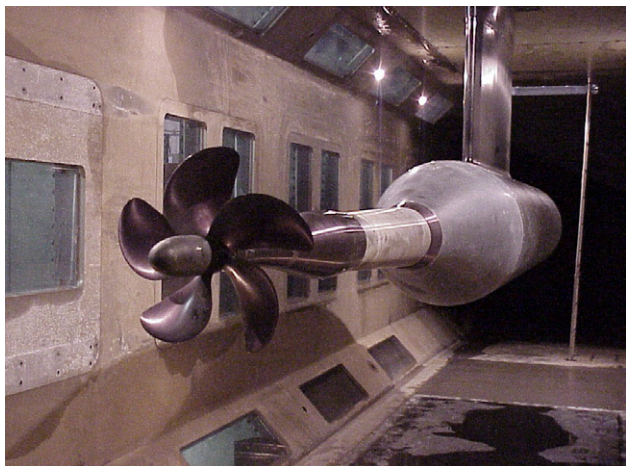


**Figure 5.** Strut-mounted testing pod as prepared for an open-water (i.e. uniform inflow) propeller test. The view is looking downstream inside the LCC test section. The test-section-access personnel hatch and ladder are visible towards the top and right of the photograph.

Laser Doppler velocimetry (LDV) is by far the most common technique used for water velocity measurements in the LCC. Two Dantec direct-backscatter LDV systems—a stationary single-component system for reference measurements and a traverse-mounted two-component system for surveys—are resident at the LCC and are described in Blanton (1995b). Recent improvements to these systems are described in Park *et al* (2002, 2003). Particle seeding for LDV purposes has been frequently unnecessary (Blanton and Etter 1995), has merely involved flood seeding the entire LCC volume with silicone carbide or titanium dioxide particles ( $1\text{--}2\ \mu\text{m}$  average size), or has involved injection of silver-coated spheres  $4\ \mu\text{m}$  in diameter from the test model (Fry 1995). The LDV test that involved the injection of the silver-coated spheres was conducted using a custom hub-mounted optical arrangement that allowed the quantification of the flow in the wake plane from within a nearly axisymmetric body that was being tested.

Particle-imaging velocimetry (PIV) has been used successfully in the LCC as well. Figure 6 shows a schematic of a recent successful PIV setup (Bourgoyne *et al* 2003) that was simple and robust. Planar velocity field measurements were made in the vicinity of the trailing edge of a hydrofoil using two digital cameras with  $1280 \times 1024$  pixel resolution and a PC-based data acquisition system. For these tests, the LCC was flood seeded with silver-coated glass spheres of  $16\ \mu\text{m}$  mean diameter and light was provided by two flash-lamp-pumped Nd-YAG lasers delivering 800 mJ per pulse at a wavelength of 532 nm. The large reflective particles and the bright laser pulses were sufficient to overcome the long optical path lengths. The laser sheet was masked to 3 mm thickness and relayed downward through the top of the LCC test section and 1.5 m of water to illuminate the foil's suction-side trailing edge and near wake. The pressure side of the hydrofoil was not illuminated. The two cameras viewed the flow horizontally through ordinary 35 mm camera lenses and approximately 1 m of water, and operated at a magnification of 0.1 mm/pixel to capture nearly side-by-side images. For these measurements, the camera's depth of field exceeded the light

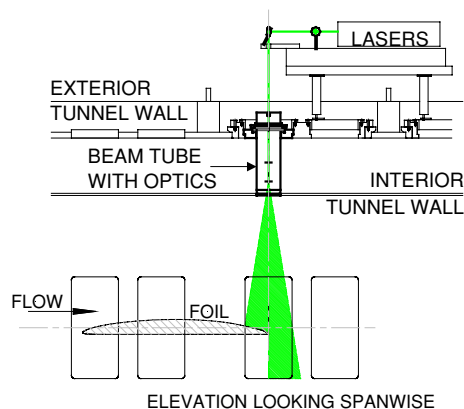


**Figure 6.** Schematic of the particle-imaging velocimetry (PIV) system recently employed at the LCC. The pulsed lasers were mounted above the test section and fired downward through 1.5 m of water. The PIV cameras viewed the flow from the prospective shown but were focused on the foil's trailing edge and near wake. The LCC test section windows, shown as rectangular outlines above, measure  $1.17\ \text{m} \times 0.54\ \text{m}$ .

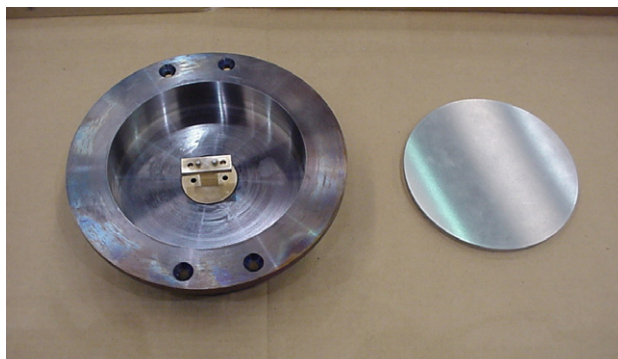


**Figure 7.** Photograph of the strain-based direct-measurement shear-stress sensor showing the sensor housing on the left with the load cell mounted in its centre, and the polished 152 mm diameter sensory surface removed and placed to the right.

sheet thickness. Raw images from the two cameras were converted to velocity vector fields by cross-correlating  $32 \times 32$  pixel interrogation areas containing on average approximately ten particle pairs. Accordingly, each resulting PIV vector arises from particle-pair averaging over a cube measuring approximately 3 mm on a side. For this study, dual pulsed images were acquired at a rate of approximately 1 Hz.

Average skin friction is one of the most difficult measurements to make in a water tunnel. Many techniques are available if indirect methods are acceptable (see Hanratty and Campell (1996) and Nagib *et al* (2004)). However, underwater force balances appear to be the only direct measurement approach for water tunnels. Successful LCC testing has been performed with strain-gauge-based floating-plate shear-stress balances designed and constructed at the Applied Research Laboratory at Pennsylvania State University. Figure 7 shows a photograph of a strain-gauge-based shear-stress sensor. The critical performance issues for these devices are the maintenance of a level-sensing surface flush with the sensor housing and a small gap around the sensing surface perimeter (Hanratty and Campell 1996). The shear-stress sensors used in the LCC were circular with a 152 mm sensor diameter and a nominal perimeter gap of  $25\text{--}75\ \mu\text{m}$ . Strains were measured

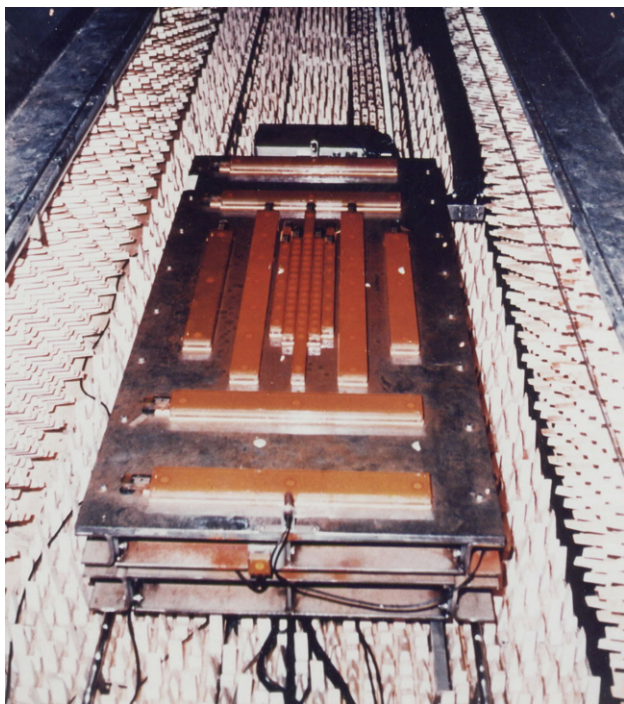


**Figure 8.** A photograph of the 95-element acoustic array and carriage in the LCC test section trough with the floor-mounted acoustic window removed.

with solid-state strain gauges on a thin metal web that spanned the gap between the two support legs of a load cell that was mounted in the interior of the housing (see figure 7). These sensors were calibrated with weights having masses of 50 g to 1.0 kg. Typical strain amplitudes were of order  $10 \mu$ -strain when these sensors were used during flat-plate turbulent boundary layer testing at nominal free-stream flow speeds between 6 and  $18 \text{ m s}^{-1}$ .

Perhaps the LCC's most unusual instrumentation is its multiple acoustic recording systems. The largest is a 95-element hydrophone array which consists of four nested sub-arrays, two high-frequency arrays and several broadband omni-directional hydrophones (see figure 8). This equipment is used typically for near-field beam forming to determine sound source locations and strengths either within or near the model in the test section. All the various arrays and hydrophones are mounted on a movable carriage, 0.6 m wide and 1.8 m long, that is housed in an acoustic trough below the test section (see figure 2). The trough is covered by an acoustic window made from rubber and aluminium that isolates the array from the test section flow while allowing static pressure equalization and sound penetration. The trough is lined with echo- and vibration-absorbing wedges to reduce reverberation and vibration. The trough is 13.7 m long, 2.1 m wide and 1.1 m deep, and extends the entire length of the test section. Thus, the 95-element array can be traversed in the streamwise direction to collect sound radiation results as a function of downstream distance. In addition to the equipment in the acoustic trough, small broadband hydrophones (100 Hz to 100 kHz) can be positioned in the acoustic trough and at 1.52 m intervals in the corner fillets at the top and bottom of the test section. And, downstream of the test section in the LCC's diffuser, a



**Figure 9.** Cavitation visualization of the interaction between a propeller wake and rudder. The propeller diameter is 40.6 cm and the rudder chord at its tip is 18.6 cm. (Photograph: courtesy of Dr Young Shen of NSWCCD.)

53 cm diameter acoustic lens and a receiving hydrophone are positioned in line with the test section centreline to acquire stern aspect radiated noise from 5 kHz to 100 kHz. All the hydrophones are connected to an acoustic data acquisition and analysis system that is capable of automatic beam forming and calibrated source-level measurements.

#### 4. Sample results from LCC tests

As might be expected, the first genuine hydrodynamic experiments in the LCC involved cavitation and focused on travelling bubble cavitation on axisymmetric head forms having diameters from 5.08 cm to 50.8 cm (Kuhn de Chizelle *et al* 1995). However, more typical cavitation tests have involved hull forms and fully operational powered models. Figure 9 is a sample photograph from a study of the cavitation that occurs when a powered propeller wake interacts with a stationary rudder. Here, the visual access of the LCC test section was critical for observing and understanding the phenomena, and developing the appropriate redesign. In this case, the addition of some twist to the rudder suppresses the formation of vapour cavities on the rudder when all the other flow conditions are held constant.

A combination of recent LDV and shear-stress measurements in the LCC is provided in figure 10 for the average streamwise velocity,  $\bar{u}(y)$ , in a near-zero-pressure-gradient flat-plate turbulent boundary layer at nominal test section flow speeds of 6, 12 and  $18 \text{ m s}^{-1}$ . In this figure,  $y$  is the vertical distance from the plate and the actual flow speeds outside the plate boundary layer were approximately 10% higher because of blockage from the 17-metric-ton test-section-spanning model that was 12.9 m long and 18.4 cm thick. The test surface of the model was polished to be hydrodynamically smooth and boundary layer growth on the model and tunnel sidewalls produced a mild favourable pressure gradient. Patel's dimensionless acceleration parameter,  $(\nu/U^2)(dU/dx)$ , was less than  $10^{-9}$  at all three test speeds. The results in figure 10 are presented with the usual dimensionless law-of-the-wall scaling that involves the fluid density  $\rho$ , fluid kinematic viscosity  $\nu$  and local skin

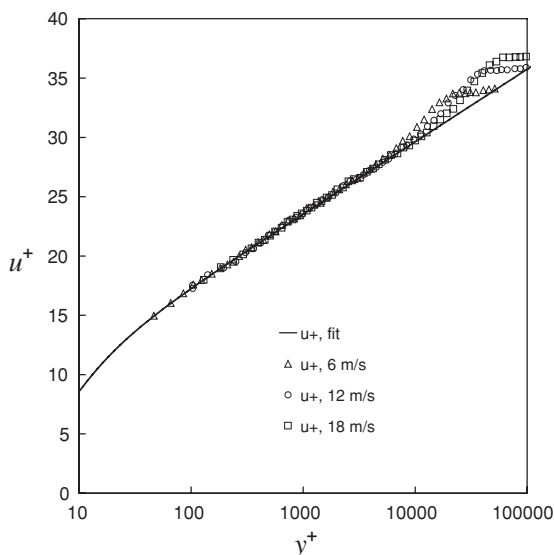


**Figure 10.** The average streamwise velocity,  $\bar{u}(y)$ , in a near-zero-pressure-gradient flat-plate turbulent boundary layer at a downstream distance of 10.7 m for nominal LCC test section flow speeds of 6, 12 and 18 m s<sup>-1</sup> using the usual law-of-the-wall dimensionless parameters:  $u^+ = \bar{u}/\sqrt{\tau_w/\rho}$  and  $y^+ = y\sqrt{\tau_w/\rho}/\nu$ , where  $y$  is the vertical distance from the plate,  $\tau_w$  is the wall shear stress,  $\rho$  is the fluid density and  $\nu$  is the water kinematic viscosity. The fit is based on Spalding's formula (see White (1991)) with von Karman constant  $\kappa = 0.38$  and intercept parameter  $B = 5.2$ . The downstream distance-based Reynolds numbers are approximately 70 million, 140 million and 210 million.

friction  $\tau_w$ . These measurements correspond to momentum-thickness-based Reynolds numbers of 66 000, 126 000 and 186 000, which lie above the Reynolds numbers of prior smooth-plate laboratory studies. The nearly two decades of the log-law displayed in figure 10 are indicative of high Reynolds number results. The Spalding fit provided in this figure uses a value of the von Karman constant ( $\kappa = 0.38$ ) that is consistent with other recent high Reynolds number turbulent boundary layer investigations (Nagib *et al* 2004). These measurements are the highest Reynolds number smooth-wall flat-plate boundary-layer profiles ever reported. As of this writing, they have not been published elsewhere and illustrate the LCC's unique capacity for high Reynolds number flow studies.

The PIV system described above was used extensively to study the Reynolds number dependence of near-wake vortex shedding from a two-dimensional hydrofoil. Near-wake vortex shedding from propeller blades and control surfaces leads to unintended tonal hydroacoustic noise and is known to be unexpectedly Reynolds number dependent. For this investigation, the solid nickel-aluminium-bronze test foil spanned the LCC test section and had a chord and maximum thickness of 2.13 m and 17 cm, respectively. The hydrofoil shape was NACA 16 modified to have a flat pressure side aft of 28% chord and a smoothly tapered trailing edge that ended in a bevel angle of either 44° or 56°. The foil was cambered and had a thickness-to-chord ratio of 8% and a camber-to-chord ratio of 3.2%. It was mounted in the LCC with the flat portion of its pressure side parallel to the on-coming free stream. The foil's entire surface was polished to a surface roughness of 0.25  $\mu\text{m}$ . At a LCC test section flow speed of 18.3 m s<sup>-1</sup> and

the nominal zero-degree angle-of-attack configuration, the foil generated 60 metric tons of lift.

Sample PIV results from this investigation are shown in figure 11 which displays two instantaneous images of spanwise vorticity fluctuation (colour contours) and the flow velocity fluctuation (vectors) at chord-based Reynolds numbers of  $Re_C = 4$  million and 50 million. The final 1% of the foil chord—showing the 56° trailing-edge bevel angle—is depicted at the left edge of both frames in figure 11. The vertical span of each figure panel,  $\pm 3\%$  of the foil's chord, corresponds to  $\sim 13$  cm. The offset and truncated rectangles of data correspond to the imaging regions of the two PIV cameras. Here, it is readily apparent that vortex shedding is prevalent at  $Re_C = 4$  million but is nearly absent at  $Re_C = 50$  million. This Reynolds number range matches that of many full-scale ship propellers and heavy-lift aircraft wings, but unique tests such as these are manageable in the LCC because of its size, support equipment and robust construction. The particular results shown in figure 11 have not been published elsewhere.

While the majority of models tested in the LCC are scaled-down versions of full-scale prototypes, some full-scale models have been tested, taking advantage of the LCC's large test section size. These have included full-scale submarine appendages, towed array configurations and torpedoes. Figure 12 shows a full-scale research torpedo in the LCC test section. This model was supported by a single strut from the LCC test top. The propulsor at the stern was powered by an internal electric motor. Power cables for the electric motor and instrument cables from the model were passed through the strut and exited the channel pressure boundary through packing glands in the test top. This is the conventional method of providing power and signals to a strut-mounted model. At the base of the strut, the model is attached through a six-component force-measuring gauge. Testing the model in the LCC provided excellent hydrodynamic and hydroacoustic information to supplement the data normally acquired on a torpedo test range. The nested acoustic arrays in the trough under the test section allowed a scan of the body from nose to tail to measure mechanical noise sources. Independent control of the flow speed and the propulsor rotation rate allowed the propulsor to operate at off-design advance coefficients not possible at the self-propelled operating condition. Extended test periods and the ability to observe cavitation and conduct flow visualization were other advantages offered by the LCC for these tests. Also visible in figure 12 are the extensive viewing windows in the test section in both the vertical sides and corner fillets previously described in section 2.

## 5. Summary and future possibilities

The William B Morgan Large Cavitation Channel (LCC) is a unique resource for high Reynolds number hydrodynamic and hydroacoustic testing. It is the largest facility of its kind in the world and has proven to be robust and flexible for both application-directed and scientific testing. Although it was designed and constructed to meet needs existing during the final decade of the cold war, it is still able to meet many modern scientific, military and even commercial objectives. Moreover, with some modification, its operating envelope

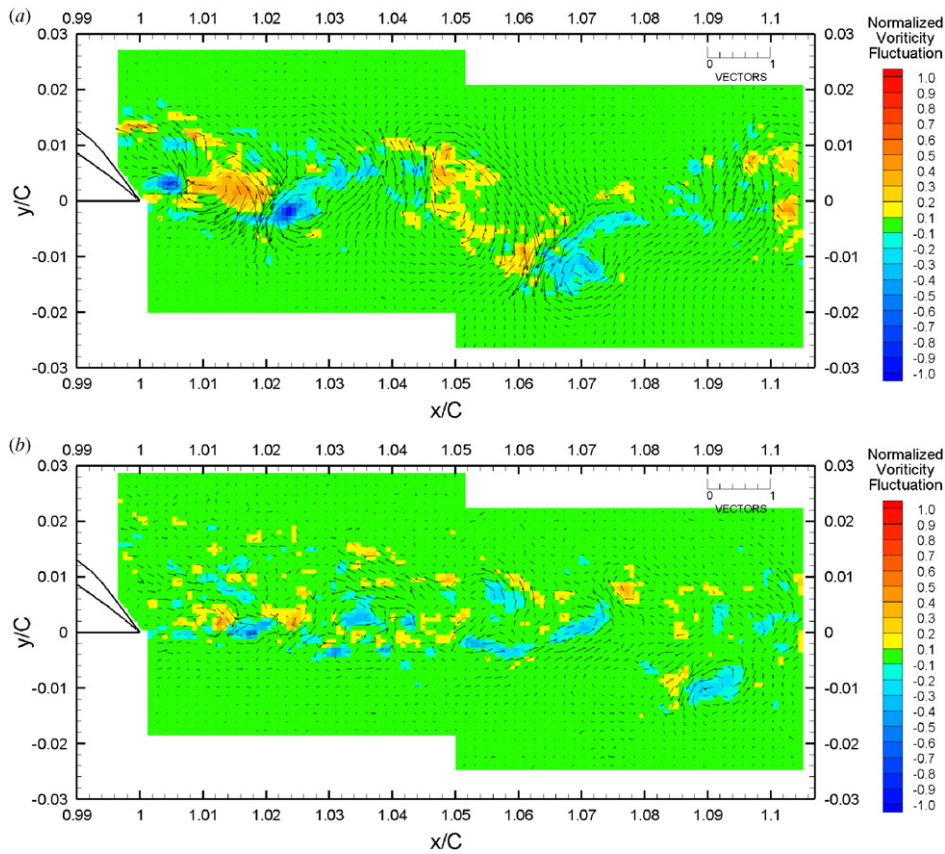


**Figure 11.** Normalized vorticity fluctuations and velocity fluctuation vectors in the near wake of a two-dimensional hydrofoil at chord-based Reynolds numbers of 4 million (a) and 50 million (b). Here,  $C$  is the foil chord (2.13 m) and the scale for the vectors is in the upper right of each frame (1 = free-stream speed). These results were obtained with the PIV system shown in figure 6. Note the greater vortex structure of the near wake at the lower Reynolds number.

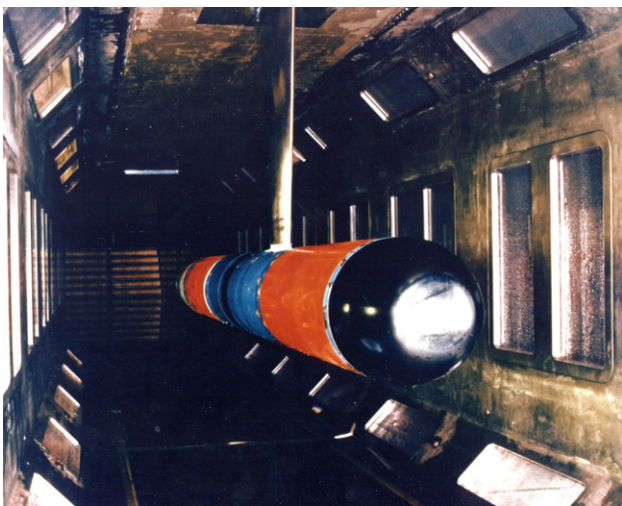


**Figure 12.** Photograph of a full-scale torpedo model mounted inside the test section on a strut attached to the LCC's test top. The view is looking downstream and the turning vanes at the end of the main diffuser, approximately 40 m away, are visible at the middle left of the image. This picture also shows the two sets of main windows at the level of the torpedo model, the four sets of corner fillet windows and the outline of the acoustic window in the test section floor.

could be expanded further. A recent performance study conducted by the authors of this paper suggests that LCC test section flow speeds of greater than  $25 \text{ m s}^{-1}$  should

be possible by replacing the existing motor with one rated to deliver approximately 25 MW of mechanical power (this figure includes a 20% reserve for model losses in the test section). Additional flow speed increases may also be possible by installing a test section liner that increases the LCC's contraction ratio and decreases its test section cross-sectional area. When higher speed testing is implemented with facility modification, structural considerations restrict the maximum test section pressure, and therefore cavitation number, to lower values.

### Acknowledgments

The authors of this paper are indebted to the many fine engineers and scientists at the Naval Surface Warfare Center who have contributed their time and talent to planning, designing, constructing and model testing at the LCC. Support for the research projects mentioned has been provided by the Office of Naval Research, the Defense Advanced Research Projects Agency and the Naval Undersea Warfare Center.

### References

Abbot P A, Celuzza S A and Etter R J 1993 The acoustic characteristics of the Naval Surface Warfare Center's Large Cavitation Channel *Proc. ASME Winter Annual Meeting (New Orleans, LA)*



- Blanton J N 1995a Uncertainty estimates of test section pressure and velocity in the Large Cavitation Channel *AIAA Paper no* 95-3079
- Blanton J N 1995b Laser Doppler velocimetry techniques in the Large Cavitation Channel *Proc. 24th American Towing Tank Conference (College Station, TX)*
- Blanton J N and Etter R J 1995 Laser Doppler velocimetry on a body of revolution in the Large Cavitation Channel *Proc. ASME Fluids Engineering Division Summer Meeting: Symposium on Laser Anemometry (Hilton Head, SC)*
- Bourgoyne D A, Hamel J A, Ceccio S L and Dowling D R 2003 Time averaged flow over a hydrofoil at high Reynolds number *J. Fluid Mech.* **496** 365-404
- Etter R J 2001 The evolution of cavitation tunnels in marine laboratories *Proc. 26th American Towing Tank Conference (Glen Cove, NY)*
- Etter R J and Wilson M B 1992 The Large Cavitation Channel *Proc. 23rd American Towing Tank Conference (New Orleans, LA)*
- Fry D J 1995 Model submarine wake survey system using internal LDV probes *Laser Anemometry—1995* vol 229 (ASME Fluids Engineering Division) pp 159-69
- Hanratty T J and Campbell J A 1996 Measurement of wall shear stress *Fluid Mechanics Measurements* 2nd edn ed R J Goldstein (Washington, DC: Taylor and Francis) chapter 9
- Kuhn de Chizelle Y, Ceccio S L and Brennan C E 1995 Observations and scaling of traveling bubble cavitation *J. Fluid Mech.* **293** 99-126
- Nagib H, Christophorou C, Reidi J-D, Monkewitz P, Österlund J and Gravante S 2004 Can we ever rely on results from wall-bounded turbulent flows without direct measurements of wall shear stress? *AIAA Paper no* 2004-392
- Park J T, Cutbirth J M and Brewer W H 2002 Hydrodynamic performance of the Large Cavitation Channel (LCC) *Naval Surface Warfare Center Technical Report NSWCCD-50-TR-2002 068*
- Park J T, Cutbirth J M and Brewer W H 2003 Hydrodynamic performance of the Large Cavitation Channel (LCC) *Proc. 4th ASME-JSME Joint Fluids Engineering Conference (Honolulu, HI)*
- Wetzel J M and Arndt R E A 1994a Hydrodynamic design considerations for hydroacoustic facilities: Part I. Flow quality *ASME J. Fluids Eng.* **116** 324-31
- Wetzel J M and Arndt R E A 1994b Hydrodynamic design considerations for hydroacoustic facilities: Part II. Pump design factors *ASME J. Fluids Eng.* **116** 332-7
- White F M 1991 *Viscous Fluid Flow* 2nd edn (New York: McGraw-Hill) p 415